ACS APPLIED MATERIALS & INTERFACES

Research Article

www.acsami.org

Magnetic Microrheology of Block Copolymer Solutions

Jin Chul Kim,[†,‡] Myungeun Seo,[†,§] Marc A. Hillmyer,*[,†] and Lorraine F. Francis*[,‡]

[†]Department of Chemistry, University of Minnesota, Minneapolis, Minnesota 55455-0431, United States

[‡]Department of Chemical Engineering and Materials Science, University of Minnesota, Minneapolis, Minnesota 55455-0132, United States

Supporting Information

ABSTRACT: The viscosity of poly(styrene)-*b*-poly(lactide) [PS-*b*-PLA] solutions in a neutral solvent was characterized by magnetic microrheology. The effect of polymer concentration on the viscosity of the block polymer solutions was compared with that of the PS and PLA homopolymers in the same solvent. The viscosity of PS-*b*-PLA solution, unlike the homopolymer solutions, showed a steep increase over a narrow concentration range. The steep rise was concomitant with microphase separation into an ordered cylindrical microstructure as determined by small-angle X-ray scattering. Hence microrheology proved effective as a means of characterizing the order−disorder transition concentration. During an in situ drying experiment, changes in local viscosity through the depth of a block copolymer solution were characterized as a function of drying time. Early in the drying process, the viscosity rose steadily and was uniform through the depth, a result consistent with steadily increasing and uniform polymer concentration. However, later in the drying process as the overall polymer concentration approached that required for microphase separation, the viscosity of the polymer solution near the free surface became an order of magnitude higher than that near the bottom of the container. The zone of high viscosity moved downward as drying proceeded, consistent with a microphase separation front.

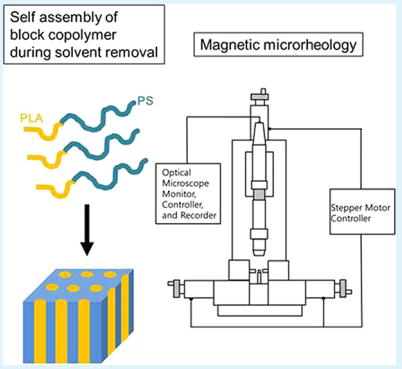

KEYWORDS: *block copolymer self-assembly, magnetic microrheology, microphase separation, PS-b-PLA, solvent removal, block copolymer dynamic viscosity, in situ drying, THF, solvent vapor annealing*

1. INTRODUCTION

Block polymers spontaneously self-assemble into periodically ordered structures with length scales usually ranging from 5 to 50 nm. Nanostructured block polymer thin films have tremendous potential for nanotechnology applications. For instance, they can serve as templates for transferring nanostructures to other substrates (block polymer lithography[1−6]) and as membranes for advanced separations.[2,7,8] In these applications, achieving the desired microphase-separated nanostructure is typically necessary.[9−11] Therefore, considerable attention has been given to developing methods to improve microstructural ordering and alignment in thin films (e.g., alignment of cylinders perpendicular to the film surface). Thin films are prepared by depositing a block polymer solution onto a substrate by spin coating or dip coating, for example, and drying to form a solid film. Typically, the film is then annealed at elevated temperature or in the presence of solvent vapor to organize the structure.[12−15] Solvent vapor annealing is more attractive than thermal annealing and provides greater flexibility in morphology control and does not cause thermal degradation.[16,17] While these annealing methods are effective, an alternative is to control the deposition and drying process so that the desired nanostructure develops directly on drying and no secondary treatment is needed. A step toward this goal is to develop a characterization tool for exploring the structure development through the thickness of a drying block polymer coating.

Microrheological methods have potential for studying the state of the block polymer film during the removal of solvent. These methods use small probe particles to characterize the rheological properties of liquids at micrometer length scales. Local viscosity changes in a drying or swollen film can indicate the emergence of an ordered state, and thus measurements of local viscosity can give insight into the organization processes associated with drying and solvent vapor annealing.[18−21] Magnetic microrheology[22−29] is particularly attractive for such a study because this noncontact method can generate large forces and therefore probe a wider viscosity range than passive microrheology methods that rely on Brownian motion.

In magnetic microrheology, a liquid specimen containing a very dilute concentration ($<10^{-4}$ vol %) of superparamagnetic probe particles is placed in a magnetic field gradient created with precisely positioned permanent magnets or electromagnets. The field gradient, dB/dx, produces a magnetic force, F_M, on the magnetic probe particle

Received: August 23, 2013
Accepted: October 28, 2013
Published: October 28, 2013

$$F_M = \frac{M}{\mu_o}\left(\frac{4\pi R^3}{3}\right)\frac{dB}{dx} \quad (1)$$

where M is the magnetization and R is the radius of the probe particle, respectively, and μ_0 is the permeability of free space. This force sets the particle into motion. A viscous drag force, F_{drag}, counters this motion

$$F_{drag} = -6\pi\eta R v \quad (2)$$

where η is the viscosity and v is the velocity of the particle. In typical experiments, other possible factors influencing the particle motion (e.g., thermal fluctuations, gravity, inertia) are negligible, and a force balance ($F_M + F_{drag} = 0$) provides a relationship between the local viscosity and the measured velocity.

$$\eta = \frac{2MR^2(dB/dx)}{9\mu_o v} \quad (3)$$

This force balance above assumes that the liquid is Newtonian. Since particle velocities are typically low and the shear rate ($\dot{\gamma} \approx v/2R$) is thus also low, this assumption is typically valid.

Magnetic microrheology has been used to characterize rheological properties of small volumes of soft biomaterials,[30−32] colloidal dispersions,[33,34] and polymers.[35−39] Recently, this method has been applied to the measurement of changes in viscosity of polymer coatings during controlled solidification.[23,40] The application of the method to structure development in block polymer solutions has not been reported.

In this study, we used a magnetic microrheometer to characterize the shear viscosity of various poly(styrene)-*b*-poly(lactide) (PS-*b*-PLA) block copolymer and PS or PLA homopolymer solutions in tetrahydrofuran. In this work we utilized a cylinder-forming PS-*b*-PLA sample and THF as solvent given the technological relevance of this system for nanopatterning applications.[41] First, the effect of polymer concentration was explored for the various polymer solutions, and the results were compared to traditional Ubbelohde viscometry. Then small-angle X-ray scattering measurements were used to establish a correlation between the microstructure and the viscosity at various concentrations for the PS-*b*-PLA solutions. Finally, the local viscosity of PS-*b*-PLA block copolymer solutions was measured in situ during solvent removal, and the results connected to the structural development.

EXPERIMENTAL SECTION

Materials. Polystyrene (PS) homopolymer (with a nominal number average molar mass, M_n = 35 kg/mol) and tetrahydrofuran (THF) (ACS reagent grade, ≥99.0%) were purchased from Sigma-Aldrich and used as-received. Independent analysis by size exclusion chromatography using PS standards revealed that this polymer exhibited a biomodal molar mass distribution with one peak at M_n = 70 kg/mol, dispersity = 2.1 and the other at M_n = 0.9 kg/mol, dispersity = 1.6. The poly(styrene)-*b*-poly(lactide) (PS-*b*-PLA) block polymer (M_n = 75 kg/mol, f_{PS} = 0.72, dispersity = 1.19) was synthesized by a combination of reversible addition−fragmentation chain transfer polymerization and ring-opening transesterification polymerization, according to a published procedure.[7] Polylactide (PLA) homopolymer (M_n = 28 kg mol^{-1}, dispersity = 1.18) was prepared by ring-opening transesterification polymerization (ROTEP).[8] Dynabead M280 tosyl-activated superparamagnetic particles (cross-linked polystyrene with 17 wt % ferrite dispersed in water; 30 beads/mL; bead density = 1.4 g/cm^3) were purchased from Life Technologies.

Magnetic Particle Characterization and Preparation. Scanning electron microscopy (SEM) was conducted on a Hitachi S-4700 FE-SEM (Schaumburg, IL) to determine the size and size distribution of superparamagnetic particles. SEM analysis of the dried particles indicated the average particle diameter of 2.83 μm with a standard deviation of 1%, consistent with the reported values in the literature[42] (see Figure S1 in the Supporting Information). Vibrating sample magnetometry (VSM) was performed on a Micro/Mag Vibrating Sample Magnetometer (Princeton Measurement Corporation, Princeton, NJ) for characterization of magnetization of superparamagnetic particles (see Figure S2 in the Supporting Information). The results showed that the saturation magnetization was 12.3 kA/m at magnetic fields greater than 0.2 T, also comparable to the literature value.[42]

The route for the dispersing magnetic particles in THF is shown Figure S3 (Supporting Information). The as-received aqueous dispersion of magnetic particles was placed in a 20 mL vial, and the particles were isolated using a magnetic separator (Biomag MultiSep Magnetic Separator, Bangs Laboratories, Inc.). After decanting the water, THF was added, and the particles were redispersed. This process was repeated several times to completely remove water in the THF dispersion. The final concentration of magnetic particles was adjusted to be 7.5 × 10^{-5} g/mL (5.4 × 10^{-3} vol %).

Preparation of Polymer Solutions at Fixed Polymer Concentration for Microrheology Experiments. Polymer solutions (10−40 wt %) containing a small quantity of magnetic particles (∼5 × 10^{-3} vol %) were prepared in custom Teflon containers (∼6 mm in height, ∼7 mm in width and length) (see Figure S4 in the Supporting Information). First, vacuum grease was applied to the top of the container, and the weight of the container was recorded. Then, solid polymer was added to the container followed by the dispersion of magnetic particles in THF, in amounts required to form the polymer solution in THF at the concentration of interest. To prevent evaporation of THF, the top of the container was covered with a preweighed glass slide and a preweighed windowed ceramic cap. The whole assembly was placed in a desiccator for 48 h prior to the microrheology experiment. Before starting the microrheology experiment, the weight of the assembly was measured to determine the final polymer concentration. If necessary, the magnetic particles were redispersed by gentle agitation. The polymer solution volume required for filling the container was 0.02 mL.

Magnetic Microrheology of Polymer Solutions. Microrheology experiments were performed on a custom-built magnetic microrheometer designed for coating research.[23] Briefly, the rheometer consists of two opposing NdFeB permanent magnets mounted on stepper motors, a sample stage, and a digital optical microscope (KH-7700, Hirox-USA, NJ) mounted on a stepper motor (see Figure 1). The gap between the two magnets was set to 15 mm, and the magnitude of the magnetic field gradient dB/dx was 47.5 T/m over the observation region of the microscope, as determined using a gaussmeter (5100 series, F.W. Bell, Orlando, FL). The magnetic field was well above that needed to completely saturate the magnetization of probe particles.

After placing the filled container on the sample stage between the two magnets, a magnetic particle was located using the microscope and tracked by capturing images at fixed time intervals. In a typical experiment, the microscope position is first adjusted so that a reference surface (e.g., bottom of vial) is in focus, and then the position of the microscope is changed using the stepper motor so that a particle comes into focus. The trajectory of the magnetic particle is then tracked by capturing the particle position at 1−30 s intervals for 0.5−30 min. For each polymer solution, measurements were made on at least 20 different particles. Images are captured at 1400× magnification with the working distance of 1.3 cm and the depth of the field of 7.6 μm. The field of view was 235 × 176 μm^2. For each image, the particle position in x−y coordinates is extracted using Image J Plug-in with 2D particle detector (v.1.41, NIH Bethesda, MD). The vertical position (z-position) of the particle relative to a reference surface is known based on motion of the stepper motor (±0.1 μm) used to bring the particle into focus. While the stepper motor has high accuracy, the z-position accuracy is limited by the depth of field (7.6 μm). Only

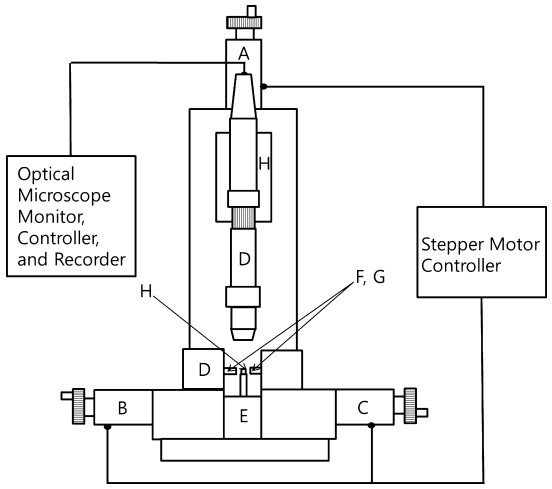

Figure 1. Microrheometer setup. A, B, and C: stepper motors. D: optical microscope (magnification: ×140−1400, working distance 13 mm). E: Sample stage. F and G: NdFeB permanent magnets. H: sample container.

particles that were at least 20 particle diameters away from the bottom and sidewalls of the container were tracked to avoid the retarding effect of solid surface on the particle motion.[43] We also made sure that the particles were a comparable distance away from the free surface of the liquid.

Capillary viscometry of polymer solutions was performed using precalibrated Ubbelhode viscometers (Cannon Instrument Company, State College, PA) at 25 °C.

In Situ Microrheology Measurement of the Viscosity during Drying of a Polymer Solution. A polymer solution (30 wt %) containing magnetic particles was prepared and transferred into a Teflon container (see Figure S4 in the Supporting Information). The container was covered with a slide glass without vacuum grease and the ceramic cap; evaporation of THF was slowed by the glass and cap (rate of weight loss was ∼0.04 mg/s initially).

The velocities of magnetic particles at different z-positions (relative to the free surface) and at different drying times were tracked. In any given experiment, several particles could be tracked by following an iterative procedure. First, a particle is found in some target region of the container. Next, the stepper motor is used to quickly adjust the microscope position to bring the free surface into focus and then return to the particle. The motion of the stepper motor establishes the z-position of the particle relative to the free surface. The particle is tracked, keeping the total tracking time to a minimum to ensure that the local composition and position relative to the surface do not change appreciably during the measurement. Then, the procedure is repeated; a new particle is found, referenced to the free surface, and then tracked. Typically, three or four particles could be tracked in the course of a 12 min drying experiment. Multiple experiments were carried out to determine the viscosity change in three target regions: 0.9 ± 0.2 mm from the free surface, 1.5 ± 0.2 mm from the free surface, and 2.0 ± 0.2 mm from the free surface. The choice of the ±0.2 mm range is based on the random distribution of magnetic particles and the searching procedure that was used. Additionally, a parallel experiment was done with a thermocouple inserted into a THF-filled vial to estimate the amount of evaporative cooling. A uniform temperature drop of about 3 °C was noted. This cooling is not expected to affect the viscosity measurement appreciably.

The motion of the free surface of the polymer solution during drying led to several effects. First, if the contact line was pinned to the container walls then a curved meniscus developed, which caused convective flows. If this situation occurred, then particles could not be tracked accurately, and the data were discarded. Fortunately, this problem was not severe for drying of the 30 wt % polymer solution. Also, the tracking time was adjusted to account for the free surface motion. Early in the drying process, the maximum tracking time for a particle was limited to 30 s to minimize error in the z-position caused by the descent of the free surface during drying (approximately 0.002 mm/s). In the later stages of drying, the drying rate dropped significantly so that this issue was no longer a concern. Near the surface, the viscosity of the polymer solution eventually became so high that the movement of the particles was too slow to be accurately measured.

Small-Angle X-ray Scattering (SAXS) of PS-*b*-PLA Solutions. SAXS samples were in Tzero hermetic aluminum pans for differential scanning calorimetry (TA Instruments, New Castle, DE). PS-*b*-PLA was loaded into a preweighed pan, and the mass of the polymer was determined. Then a designated amount of THF was added using a micropipet, and the pan was sealed with a preweighed cap using a Tzero press. The amount of THF was accurately determined by subtracting the mass of (pan + polymer + cap) from the mass of the sealed pan. The samples were equilibrated for several days at room temperature before the SAXS measurements. PS-*b*-PLA samples without THF were also prepared and annealed in the TA Q20 DSC at 150 °C for 5 h and slowly cooled to room temperature (2 °C/min). Polymer samples without solvent were also prepared and annealed in the TA Q20 DSC at 150 °C for 5 h and slowly cooled to 25 °C (2 °C/min). SAXS experiments were performed at the Advanced Photon Source (APS) at Argonne National Laboratories at Sector 5-ID-D beamline, using a wavelength of 0.73 Å and sample to detector distance of 4.6 or 4.0 m. Scattering intensity was monitored by a Mar 165 mm diameter CCD detector with 2048 × 2048 pixels. The two-dimensional scattering patterns were azimuthally integrated to afford one-dimensional profiles presented as scattering vector (q) versus scattered intensity, where the magnitude of scattering vector is given by $q = (4\pi/\lambda)\sin\theta$.

RESULTS AND DISCUSSION

Table 1 gives the velocities of magnetic particles measured in the microrheometer for PS and PLA solutions of various concentrations. During the measurement, no aggregation or interaction of magnetic probe particles in the polymer solution was observed. The measured particle velocities ranged from ∼0.1 to 100 μm/s with standard deviations less than 10%. Sedimentation did not interfere with the measurement; the sedimentation velocity, calculated by Stokes law, was at least 4 orders of magnitude lower than the measured velocity due to the magnetic field gradient. Shear rates determined by the ratio of the velocity to the particle diameter ($\dot{\gamma} \approx v/2R$) ranged from 0.1 to 34 s^{-1}. Under these low shear rates, the polymer solution

Table 1. Particle Velocity and Viscosity of PS and PLA THF Solutions from Microrheology

	PS		PLA	
polymer wt %	particle velocity (μm/s)	viscosity[a] (mPa·s)	particle velocity (μm/s)	viscosity[a] (mPa·s)
10	95.5 ± 5.6	2.73 ± 0.20	47.4 ± 2.8	5.46 ± 0.40
20	28.1 ± 1.7	9.27 ± 0.66	9.54 ± 0.60	27.3 ± 1.9
30	9.31 ± 0.85	28.0 ± 1.3	1.78 ± 0.09	146 ± 13
40	2.67 ± 0.16	97.6 ± 7.0	0.33 ± 0.02	780 ± 52

[a]Calculated with eq 3.

is Newtonian, as discussed more below, and the shear viscosity was calculated using eq 3. These calculated viscosities are shown in Table 1.

A comparison of the viscosities of the PS and PLA homopolymer solutions measured by a microrheometer with the values determined by Ubbelohde viscometry is presented in Figure 2. For PS and PLA homopolymer solutions, the increase

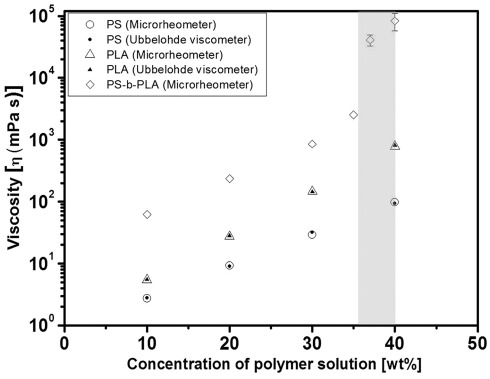

Figure 2. Effect of concentration on viscosity of PS (M_n = 35 kg/mol), PLA (M_n = 28 kg/mol), and PS-*b*-PLA (M_n = 75 kg/mol, f_{PS} = 0.72) solutions in THF at 298 K. The error ranges are determined by standard deviation for measurements of 20 probe particles. Gray region denotes order−disorder transition concentration of PS-*b*-PLA solution characterized by SAXS measurement.

in viscosity with solution concentration follows typical behavior for polymers in good solvents. The values obtained from the two different measurements agree well (i.e., within 5%) over the entire range. The shear rates of Ubbelhode viscometry can be determined from[44]

$$\dot{\gamma} = \frac{4V}{\pi r^3 t} \quad (4)$$

where V is efflux volume; r is capillary radius; and t is efflux time. For our experiments, the calculated shear rates are in the range 7.08−672 s^{-1}. For a given polymer solution, the shear rate for the Ubbelhode viscometer measurement is greater than that for microrheometer measurement (for details, see Table S1 in the Supporting Information); however, the viscosities determined by the two methods are in near perfect agreement. This is consistent with Newtonian behavior at these shear rates. For both methods, the shear rates experienced by the more concentrated, higher viscosity solutions were at the low end of the shear rate ranges cited. Since the critical shear rate for a transition from Newtonian to non-Newtonian behavior decreases with increasing polymer concentration, the preservation of Newtonian behavior for all solutions is reasonable.

Table 2 shows particle velocities and calculated viscosities for PS-*b*-PLA solutions as a function of concentration. For solutions with up to 35 wt % polymer, the data show good reproducibility with a low variation in the measured velocities (<10%). Shear rates were also low (e.g., 0.04 s^{-1} for 35 wt % solution); therefore, the block polymer solutions were considered Newtonian, and shear viscosity was calculated from eq 3. However, for the two highest concentrations, 37 and 40 wt %, the particle velocities are dramatically lower, and the variability is much greater. For these high viscosity liquids, the movement of the probe particles frame by frame was very small, generating errors in the tracking, which is based on following the center position of the particles. Similar errors were found in

Table 2. Particle Velocity and Viscosity of PS-*b*-PLA Solution (THF) from Microrheology

	PS-*b*-PLA	
polymer wt %	particle velocity (nm/s)	viscosity[a] (Pa·s)
10	4170 ± 380	0.0625 ± 0.0029
20	1110 ± 150	0.24 ± 0.02
30	292 ± 28	0.85 ± 0.04
35	101 ± 6	2.52 ± 0.07
37	6.4 ± 2.1	41 ± 8
40	3.1 ± 1.5	83 ± 26

[a]Calculated with eq 3.

measuring the viscosity of a solution of high molar mass PS (M_n = 400 kg/mol) in THF (40 wt %), which has a similar viscosity to 35−40 wt % PS-*b*-PLA solutions (see Figure S5 in the Supporting Information). We anticipate that this problem can be overcome by using higher magnetization particles or higher magnetic field gradients. Although the shear rates were extremely low (~0.002 s^{-1}), the Newtonian assumption for these high concentration block polymer solutions is an approximation. As discussed below, these compositions are microphase separated and are best characterized as viscoelastic.

For PS-*b*-PLA solutions with concentrations up to 35 wt %, the viscosity increases moderately with concentration, similar to the increase noted for PS and PLA homopolymer solutions, but a steep (~16-fold) viscosity increase is observed for the next higher concentration tested (37 wt %). This dramatic viscosity change appears to be linked to the order−disorder transition (ODT) of the block copolymer solution. Solution X-ray small-angle scattering (SAXS) experiments support this conclusion (Figure 3). At a polymer concentration of at 33.9 wt %, a broad scattering peak centered at q = 0.15 nm^{-1} appears, consistent with a block polymer solution without long-range order. Between 35.8 wt % and 39.3 wt %, the first-order scattering peak becomes much sharper, and finally higher-order scattering peaks appear at 45.8 wt % indicating emergence of an ordered

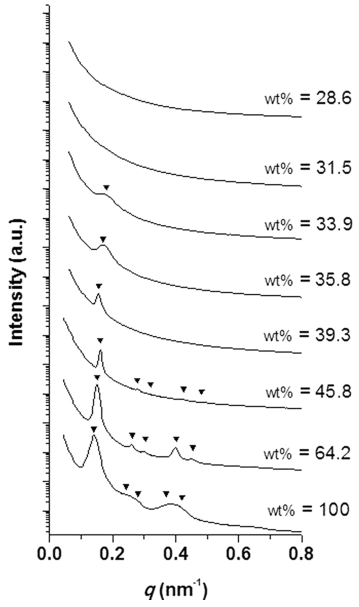

Figure 3. Small-angle X-ray scattering profiles for PS-*b*-PLA solutions at various concentrations in weight percent (wt %) of polymer in THF at 298 K.

microphase-separated structure with a hexagonally organized cylindrical microstructure. The domain spacing is ca. 40 nm around at 33.9 wt %; this structural length scale is much smaller than the size of the magnetic probe particle (~2.8 μm).

The connection between shear viscosity and block polymer solution structure found with microrheology is consistent with previous research. Dynamic or oscillatory rheology is commonly used to find the ODT of block polymer melts and solutions.[45,46] A parallel plate fixture is used, and the storage and loss moduli, G' and G'', respectively, are measured using a low amplitude oscillation at fixed frequency as the temperature is slowly increased. The low amplitude is chosen so that linear viscoelasticity applies, and the low frequency is chosen to probe microstructure rather than chain dynamics. During a temperature sweep, G' drops sharply at the ODT, indicating a loss in elasticity during disordering. The measurement conditions are chosen to prevent large disruption to the block polymer material. In fact, larger amplitude oscillations are known to increase the degree of microstructural ordering. Therefore, rheological characterization of block copolymers and block copolymer solutions under steady shear flow using techniques such as capillary rheometery or rotating spindle rheometery are rare. We could find no reports of the use of these methods to characterize the order−disorder transition in block copolymer solutions. It is interesting that the microrheology results presented here show an abrupt change in the shear viscosity coincident with microphase separation. Apparently, the localized shear of the moving magnetic particle does not compromise the ability of the method to detect the structure change associated with microphase separation.

In addition to its ability to detect the order−disorder transition, microrheology has other advantages. It is an efficient method for characterizing the viscosity of a small quantity of polymer solution. Also, the closed container setup limits complications from evaporation. Lastly, as a local viscosity measurement tool, microrheology can be used to investigate the viscosity−depth profile of polymer solution during solvent removal.

Figure 4 shows viscosity of a 30 wt % PS-*b*-PLA solution as a function of drying time and position through the depth of the solution. In the early drying stage, the overall concentration and viscosity of polymer solution gradually increase as solvent evaporates. Initially, the viscosity of the polymer solution is uniform through the depth. At 350 s, the viscosity was determined to be 2.6 Pa·s, which corresponds to ~35 wt % polymer solution based on isoconcentration viscosity measurement (see Table 2) and weight loss measurements (see Figure S6 in the Supporting Information). As noted in Figure 2, this concentration is close to the ODT. After 400 s, a significant viscosity gradient through the depth is observed. At this time point, the overall concentration of the polymer solution has risen to ~36 wt %. The viscosity near the solution surface increases quickly (open circles) with drying time. In contrast, the viscosity of polymer solution near the substrate (open triangles) remains nearly constant. After about 500 s of drying, the velocity of magnetic particles near the surface was too low to be measured, indicating a high local viscosity.

Concentration gradients are expected during the drying of polymer coatings.[47−50] Evaporation leads to an increase in the polymer concentration near the surface. If diffusion is fast enough, then the concentration through the thickness can remain uniform, but if the evaporation rate is high and/or diffusion slow, then the high concentration of polymer near the surface persists. Hence, one expects to find a viscosity gradient through the thickness. In this study a significant viscosity gradient does not occur until later in the drying process, suggesting that a relatively uniform concentration is maintained early due to facile diffusion. However, as solvent removal continues and polymer concentration climbs later in the drying process, the diffusion coefficient plummets, which would lead to a greater likelihood of a persistent concentration gradient. The appearance of the viscosity gradient in the drying specimen is coincident with the approach to the ODT composition at the probe temperature. The data suggest that a layer of high viscosity material, presumably the microphase-separated polymer solution, forms at the surface. The observed drop in the evaporation rate is consistent with the action of this layer as a "skin", slowing the diffusion of solvent to the surface; additionally, the slowing evaporation may be affected by a drop in the equilibrium vapor pressure for THF as polymer concentration at the free surface increases.[47−50] The thickness of this high viscosity layer increases as drying continues, suggesting a propagating microphase-separating front as discussed by Phillip et al.[16] Such a progression has also been suggested by other researchers,[18−21] but this report documents the change directly.

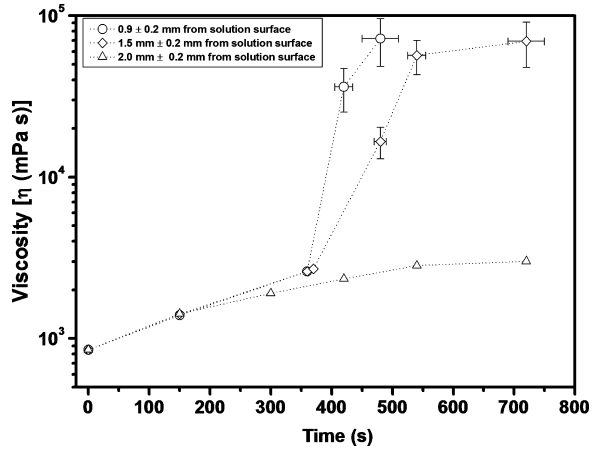

Figure 4. Viscosity changes of a 30 wt % PS-*b*-PLA (M_n = 75 kg/mol, f_{PS} = 0.72) during in situ drying conditions at 298 K. Average evaporation speed of polymer solution until 450 s was 0.04 mg/s. After 450 s, the evaporation rate rapidly dropped and fluctuated. The *y*-axis error ranges are determined by standard deviation for measurements of 10 probe particles. The dashed line was added to show the trends in the data.

SUMMARY AND OUTLOOK

In summary, we investigated the relationship between microstructure evolution and viscosity change of PS-*b*-PLA solutions in THF using magnetic microrheology. In isoconcentration experiments, a steep increase in viscosity was observed at a critical solution concentration that was consistent with the order−disorder transition, based on SAXS data. Magnetic microrheology is a viable method for identifying the ODT concentration in block copolymer solutions. Changes in local viscosity of a block copolymer solution during the solvent removal process were also characterized by monitoring magnetic particle trajectories at different distances from the free surface during drying. The data show that microphase separation of PS-*b*-PLA starts from the solution surface and propagates towards the substrate during drying. Magnetic

microrheology is a versatile tool for investigating the viscosity of small sample block polymer solutions and microphase separation.

The application of microrheology to following viscosity during drying presents more challenges as well as opportunities. The method is time intensive with an iterative approach to finding and tracking particles at various positions through the thickness of a vial of polymer solution during evaporation. To improve the success rate on these experiments, a method to prevent contact lines from pinning on container walls is needed along with an independent means of tracking the free surface position during the experiment, which would allow the spatial resolution through the thickness to be limited by the depth of field ($\pm$7.5 μm). Additionally, an improved magnet setup, employing adjustable electromagnets, would allow better control of the magnetic field gradient and hence the driving force for particle motion. Ramping up the magnetic field gradient during drying as the viscosity rises would allow data to be collected from a single particle to be tracked throughout drying, which would increase the amount of data that could be collected in a single experiment. With these improvements, monitoring the viscosity gradients in drying block polymer solution coatings with initial thicknesses on the order of 100 μm should be possible, especially with a system based on a low volatility solvent. Together with complementary interfacial rheology methods,[31,51] microrheology has great potential for enhancing the understanding of structure development in block polymer thin films.

■ ASSOCIATED CONTENT

Supporting Information

Additional figures and table. This material is available free of charge via the Internet at http://pubs.acs.org.

■ AUTHOR INFORMATION

Corresponding Authors

*E-mail: hillmyer@umn.edu.

*E-mail: lfrancis@umn.edu.

Present Address

[§]Graduate School of Nanoscience and Technology, KAIST, Daejeon 305-701, Korea.

Notes

The authors declare no competing financial interest.

■ ACKNOWLEDGMENTS

This work was supported primarily by the National Science Foundation through the University of Minnesota MRSEC under Award Number DMR-0819885. Part of this work was carried out in the College of Science and Engineering Characterization Facility, University of Minnesota, which has received capital equipment funding from the NSF through the UMN MRSEC program. SAXS data were acquired at the DuPont-Northwestern-Dow Collaborative Access Team (DND-CAT) located at Sector 5 of the Advanced Photon Source (APS). DND-CAT is supported by E.I. DuPont de Nemours & Co., The Dow Chemical Company, and Northwestern University. Use of the APS, an Office of Science User Facility operated for the U.S. Department of Energy (DOE) Office of Science by Argonne National Laboratory, was supported by the U.S. DOE under Contract No. DE-AC02-06CH11357. We thank Dr. Jin-Oh Song for useful comments and discussion. Also, we are grateful to Christopher J. Murphy and Chun-hao Lin for preparation of SAXS samples and Robert Lade, Jr. for assistance and discussion.

■ REFERENCES

(1) Urade, V. N.; Wei, T. C.; Tate, M. P.; Kowalski, J. D.; Hillhouse, H. W. *Chem. Mater.* **2007**, *19*, 768−777.

(2) Park, S.; Wang, J.-Y.; Kim, B.; Xu, J.; Russell, T. P. *ACS Nano* **2008**, *2*, 766−772.

(3) Rodwogin, M. D.; Spanjers, C. S.; Leighton, C.; Hillmyer, M. A. *ACS Nano* **2010**, *4*, 725−732.

(4) Ruiz, R.; Kang, H.; Detcheverry, F. A.; Dobisz, E.; Kercher, D. S.; Albrecht, T. R.; De Pablo, J. J.; Nealey, P. F. *Science* **2008**, *321*, 936−939.

(5) Segalman, R. A.; McCulloch, B.; Kirmayer, S.; Urban, J. J. *Macromolecules* **2009**, *42*, 9205−9216.

(6) Lee, J. I.; Cho, S. H.; Park, S. M.; Kim, J. K.; Yu, J. W.; Kim, Y. C.; Russell, T. P. *Nano Lett.* **2008**, *8*, 2315−2320.

(7) Seo, M.; Hillmyer, M. A. *Science* **2012**, *336*, 1422−1425.

(8) Yang, S. Y.; Yoon, J. H.; Ree, M.; S. K. Jang, S. K.; Kim, J. K. *Adv. Funct. Mater.* **2008**, *18*, 1371−1377.

(9) Meuler, A. J.; Hillmyer, M. A.; Bates, F. S. *Macromolecules* **2009**, *42*, 7221−7250.

(10) Yamamura, M.; Nishio, T.; Kajiwara, T.; Adachi, K. *Drying Technol.* **2001**, *19*, 1397−1410.

(11) Lee, M.; Park, J. K.; Lee, H. S.; Lane, O.; Moore, R. B.; McGrath, J. E.; Baird, D. G. B. *Polymer* **2009**, *50*, 6129−6138.

(12) Albert, J. N. L; Young, W. −S.; Lewis, R. L., III; Bogart, T. D.; Smith, J. R.; Epps, T. H., III *ACS Nano* **2012**, *6*, 459−466.

(13) Huang, H.; Hu, Z.; Chen, Y.; Zhang, F.; Gong, Y.; He, T.; Wu, C. *Macromolecules* **2004**, *37*, 6523−6530.

(14) Heinzer, M.; Han, S.; Martin, S.; Pople, J. A.; Martin, S. M.; Baird, D. G. *Polymers* **2012**, *53*, 3331−3340.

(15) Heinzer, M. J.; Han, S. L.; Pople, J. A.; Baird, D. G.; Martin, S. M. *Macromolecules* **2012**, *45*, 3471−3479.

(16) Philip, W. A.; O'Neill, B. O.; Rodwojin, M.; Hillmyer, M. A.; Cussler, E. L. *ACS Appl. Mater. Interfaces* **2010**, *2*, 847−853.

(17) Sintural, C.; Vayer, M.; Morris, M.; Hillmyer, M. A. *Macromolecules* **2013**, *46*, 5399−5415.

(18) Philip, W. A.; Hillmyer, M. A.; Cussler, E. L. *Macromolecules* **2010**, *43*, 7763−7770.

(19) Kim, S. H.; Misner, M. J.; Xu, T.; Kimura, M.; Russell, T. P. *Adv. Mater.* **2004**, *16*, 226−231.

(20) Bang, J.; Jeong, U.; Ryu, D. Y.; Russell, T. P.; Hawker, C. J. *Adv. Mater.* **2009**, *21*, 4769−4792.

(21) Sakurai, S. *Polymer* **2008**, *49*, 2781−2796.

(22) Neuman, K. C.; Nagy, A. *Nat. Methods* **2008**, *5*, 491−505.

(23) Song, J.-O; Henry, R. M.; Jacobs, R. M.; Francis, L. F. *Rev. Sci. Instrum.* **2010**, *81*, 093903−93903-8.

(24) Bausch, A. R.; Ziemann, F.; Boulbitch, A. A; Jacobson, K.; Sackmann, E. *Biophys. J.* **1998**, *75*, 2038−2049.

(25) Keller, M.; Schilling, J.; Sackmann, E. *Rev. Sci. Instrum.* **2001**, *72*, 3626−3634.

(26) Gosse, C.; Croquette, V. *Biophys. J.* **2002**, *82*, 3314−3329.

(27) Amblard, F.; Yurke, B.; Pargellis, A.; Leibler, S. *Rev. Sci. Instrum.* **1996**, *67*, 818−827.

(28) Haber, C.; Wirtz, D. *Rev. Sci. Instrum.* **2000**, *71*, 4561−4570.

(29) Lewis, J. L.; Burns, S. M.; Samuels, S. J.; Powell, P. L.; Katz, D. F. *Rev. Sci. Instrum.* **1994**, *65*, 3268−3275.

(30) Chevry, L.; Colin, R.; Abou, B.; Berret, J.−F. *Biomaterials* **2013**, *34*, 6299−6305.

(31) Choi, S. Q.; Steltenkamp, S.; Zasadzinski, J. A.; Squires, T. M. *Nat. Commun.* **2011**, *2*, 312.

(32) Weighs, D.; Mason, T. G.; Teitell, M. A. *Biophys. J.* **2006**, *91*, 4296−4305.

(33) Carpen, I. C.; Brady, J. F. *J. Rheol.* **2005**, *49*, 1483−1502.

(34) Sriram, I.; Furst, E. M. *J. Rheol.* **2009**, *53*, 357−381.

(35) Breedveld, V.; Pine, D. J. *J. Mater. Sci.* **2003**, *38*, 4461−4470.

(36) Slopek, R. P.; McKinley, H. K.; Henderson, C. L.; Breedveld, V. *Polymer* **2006**, *47*, 2263−2268.

(37) Oppong, F. K.; Rubatat, L.; Frisken, B. J.; Bailey, A. E.; De Bruyn, J. R. *Phys. Rev. E* **2006**, *73*, 041405−031405-9.
(38) Seiffert, S.; Lorenzo, F. D. *Macromolecules* **2013**, *46*, 1962−1972.
(39) Nartita, T.; Mayumi, K.; Ducouret, G.; Hébraud, P. *Macromolecules* **2013**, *46*, 4174−4183.
(40) Song, J. −O.; McCormick, A. V.; Francis, L. F. *Macromol. Mater. Eng.* **2013**, *298*, 145−152.
(41) Baruth, A.; Rodwogin, M. D.; Shankar, A.; Erickson, M. J.; Hillmyer, M. A.; Leighton, C. *ACS Appl. Mater. Interfaces* **2011**, *3*, 3472−3481.
(42) Fonnum, G.; Johansson, C.; Molteberg, A.; Mørup, S.; Aksnes, E. *J. Magn. Magn. Mater.* **2005**, *293*, 41−47.
(43) Chang, I.-D. *Angew. Z. Math. Phys.* **1961**, *12*, 6−14.
(44) Cannon Instrument Inc. http://www.cannoninstrument.com/Shear%20Rate%20Data.pdf (accessed July 2, 2013).
(45) Lodge, T. P.; Hanley, K. J.; Pudil, B.; Alahapperuma, V. *Macromolecules* **2003**, *36*, 816−822.
(46) Fredrickson, G. H.; Bates, F. S. *Annu. Rev. Mater. Sci.* **1996**, *26*, 501−550.
(47) Cairncross, R. A.; Francis, L. F.; Scriven, L. E. *Drying Technol.* **1992**, *10*, 893−923.
(48) Vinjamur, M.; Cairncross, R. A. *AIChE J.* **2002**, *48*, 2444−2458.
(49) Doumenc, F.; Guerrier, B. *Langmuir* **2010**, *26*, 13959−13967.
(50) Price, P. E.; Cairncross, R. A. *J. Appl. Polym. Sci.* **2000**, *78*, 149−165.
(51) Dhar, P.; Cao, Y.; Fisher, T. M.; Zasadzinski, J. A. *Phys. Rev. Lett.* **2010**, *104*, 016001−016001-4.